

**Photometric Observations of Soils and Rocks at the Mars Exploration Rover Landing Sites.** J.R. Johnson<sup>1</sup>, R.A. Arvidson<sup>2</sup>, J.F. Bell III<sup>3</sup>, W. Farrand<sup>4</sup>, E. Guinness<sup>2</sup>, M. Johnson<sup>3</sup>, K.E. Herkenhoff<sup>1</sup>, M. Lemmon<sup>5</sup>, R.V. Morris<sup>6</sup>, F. Seelos IV<sup>2</sup>, J. Soderblom<sup>3</sup>, L. Soderblom<sup>1</sup>, S. Squyres<sup>3</sup>, and M. Wolff<sup>7</sup>, and the Athena Science Team, <sup>1</sup>U.S. Geological Survey, 2255 N. Gemini Dr., Flagstaff, AZ 86001, jrjohnson@usgs.gov, <sup>2</sup>Washington University, St. Louis, MO, <sup>3</sup>Cornell University, Ithaca, NY, <sup>4</sup>Space Sciences Institute, Boulder, CO, <sup>5</sup>Texas A&M University, College Station, TX, <sup>6</sup>Johnson Space Center, Houston, TX, <sup>7</sup>Space Sciences Institute, Brookfield, WI.

**Introduction:** The Panoramic Cameras (Pancam) on the Spirit and Opportunity Mars Exploration Rovers [1] have acquired multispectral reflectance observations of rocks and soils at different incidence, emission, and phase angles that will be used for photometric modeling of surface materials. Phase angle coverage at both sites extends from  $\sim 0^\circ$  to  $\sim 155^\circ$ .

**Observations.** Spirit has made observations at 4 locations in the Gusev plains pointed along the antisunset and antisunrise directions (photometric equator, "PE") at 2-3 times per day. On two occasions these data sets were complemented by measurements pointed in orthogonal directions. At the rim of "Bonneville" crater, observations of the crater rim and interior were made at 5 times of day and were supplemented by images acquired as part of crater panoramas at 4 other times of day. Observations in the Columbia Hills were acquired at 3 times of day along the PE near the rock Clovis and 3 times near the rock Palenque.

At the Opportunity landing site, 3 sets of measurements were acquired along the PE within the confines of "Eagle" crater, encompassing soils and outcrop materials. These were supplemented by two near-field, targeted observations of regions containing many hematite-rich spheroidal granules. Additional images were acquired in the plains between "Eagle" and "Endurance" craters at 4 times of day along the PE and at orthogonal directions. Photometric imaging within Endurance Crater included observations of the interior dunes and rocks near Burns Cliff (Wopmay, Tipuna). Additional imaging along the PE was acquired at 4 times of day at two locations near the heatshield.

**Analyses.** In this preliminary study regions of interest among several types of soil and rock units were selected from Sol 13 sequences on Spirit (**Figure 1**) and Sol 11 sequences on Opportunity (**Figure 3**) for comparison of photometric properties. Ratios and color composites of images acquired under different phase angles in these figures demonstrate the spatial variations of the relative scattering properties among different materials. Local incidence angles for these regions (derived from stereo images [2]) were used to convert calibrated I/F values to reflectance relative to a Lambertian surface ( $R^*$ ). Phase angles for regions of interest were also extracted, allowing comparison of phase curves among units at different wavelengths. Phase angles for these sequences vary from  $20\text{-}120^\circ$  for

Spirit (**Figure 2**) and  $50\text{-}110^\circ$  for Opportunity (**Figure 4**). These curves (annotated with quadratic fits to help visualize overall trends) reveal increasing reflectance at lower phase angles associated with the backscattering lobe, and increasing reflectance at higher phase angles (forward scattering), particularly for smooth rock facets and drift materials (in hollows). For example, the phase angle coverage in Figure 2 suggests that the Spirit site's dusty ("red") rocks are relatively backscattering, soils are more isotropic, whereas drift materials and less dusty ("gray") rocks are more forward scattering, consistent with a relatively smoother surface. At the Opportunity landing site, the smooth airbag bounce marks are slightly more forward scattering than the more isotropic undisturbed soils, whereas outcrop rocks are even more forward scattering (Figure 4). Slight wavelength variations observed in the phase curves will be studied further.

**Future work.** Data extracted from the image sets described here will be corrected for diffuse/direct skylight using an atmospheric sky model based on opacity variations during the mission [e.g., 3-6]. These corrected reflectances will be used in a Hapke radiative transfer model to compare photometric properties (e.g., single scattering albedo, phase function parameters, macroscopic roughness) of different target materials to each other and materials at the Mars Pathfinder and Viking landing sites [7,8]. Additional observations of the dust-coated rover deck and calibration targets on both rovers are being investigated separately [cf. 9].

**References:** [1] Bell, J.F. III et al. *Science*, 305, 800-806, 2004; Squyres, S. et al. *Science*, 305, 794-799, 2004; Bell, J.F. III et al., *Science*, 1703-1709, 306, 2004; Squyres, S.W. et al., *Science*, 1698-1703, 306, 2004; [2] Soderblom, J. et al., *Eos Trans. AGU*, 85(47), P21A-0198, 2004; [3] Tomasko, M.G. et al., *J. Geophys. Res.*, 104, 8987-9008, 1999; [4] Smith, P.H., and M.T. Lemmon, *JGR*, 104, 8975-8986, 1999; [5] Thomas, N. et al., *JGR*, 104, 8795-8808, 1999; [6] Lemmon et al., *Science*, 306, 1753, 2004; [7] Hapke, B., Cambridge University Press, 455 pp., 1993; [8] Huck, F.O. et al., *JGR*, 82, 4401-4411, 1977; Arvidson, R.E., et al., *JGR*, 94, 1573-1587, 1989; Arvidson, R.E. et al., *Rev. Geophys.*, 27, 39-60, 1989; Guinness, E.A. et al., *JGR*, 84, 8355-8364, 1979; Guinness, E.A., *JGR*, 86, 7983-7992, 1981; Johnson et al., *JGR*, 104, 8809-8830, 1999; [9] Johnson, J.R., et al., *Icarus*, 171, 546-556, 2004; Sohl-Dickstein, J., et al., this volume; Guinness, E. et al., this volume.

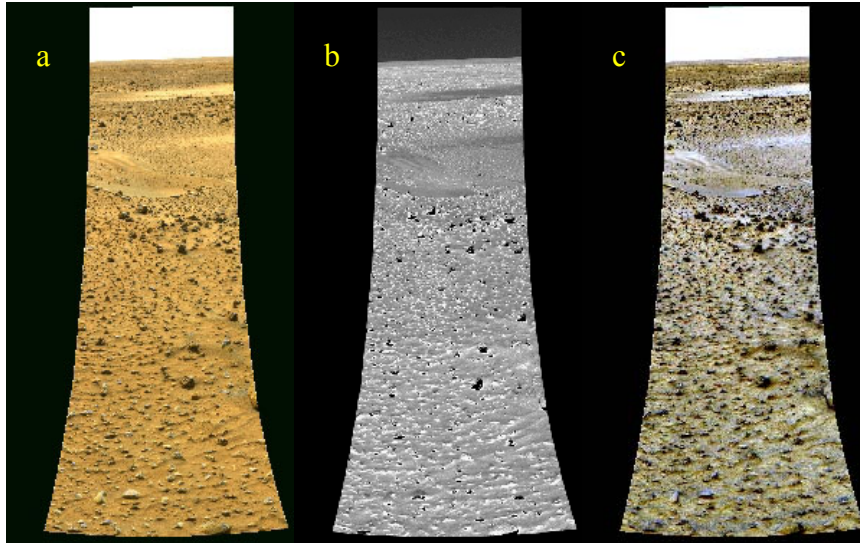


**Figure 1.** (a) False-color mosaic acquired at 1419 LTST on Sol 13 at Spirit landing site looking to the west (red=753nm, green=601nm, blue=432nm); (b) Ratio of 1053 LTST/1419 LTST 753 nm mosaics, showing forward scattering materials as darker (shadows masked); (c) False-color composite of 753 nm images acquired at: red= 1053 LTST, green = 1148 LTST, blue = 1419 LTST. In this presentation, more forward scattering materials are blue, whereas backscattering materials are red.

**Figure 2.** Phase curves (and quadratic fits) at 432 nm and 753 nm for rock and soil units from Figure 1 sequence. Error bars represent variations within selected regions of interest.

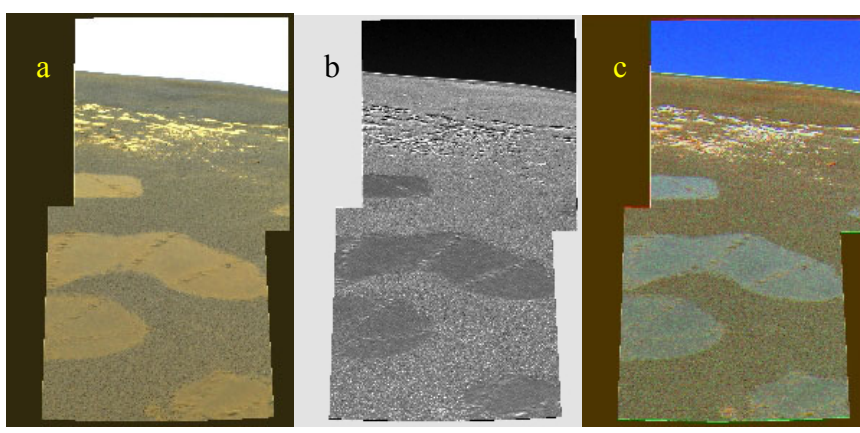
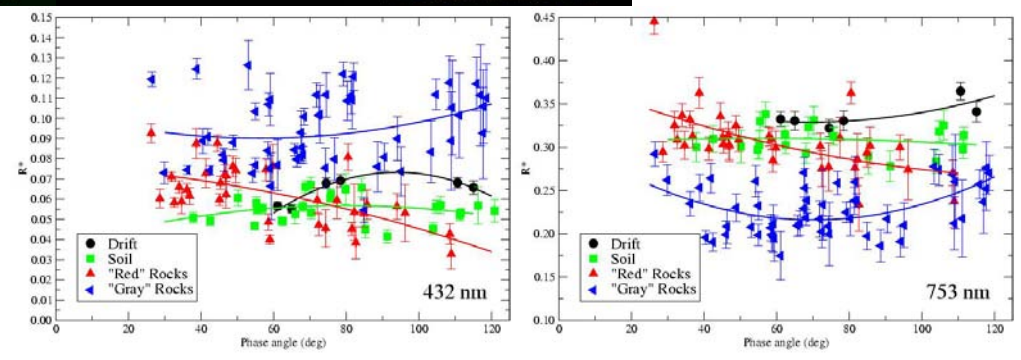


**Figure 3.** (a) False-color mosaic acquired at 1344 LTST on Sol 11 at Opportunity landing site looking to the west (red=753nm, green=601nm, blue=432nm); (b) Ratio of 1048 LTST/1344 LTST 753 nm mosaics, showing more forward scattering materials as dark; (c) Decorrelation stretch of 753 nm images acquired at: red=1048 LTST, green=1139 LTST, blue=1344 LTST; more forward scattering materials are blue.

**Figure 4.** Phase curves (and quadratic fits) at 432 nm and 753 nm for outcrop, bounce marks, and soils from Figure 3 sequence. Error bars represent variations within selected regions of interest.

